Published for SISSA by Springer

Received: July 27, 2016
Accepted: August 24, 2016
Published: August 29, 2016

# Building a holographic superconductor with a scalar field coupled kinematically to Einstein tensor

**Xiao-Mei Kuang**[a] **and Eleftherios Papantonopoulos**[b]

[a] *Instituto de Física, Pontificia Universidad Católica de Valparaíso, Casilla 4059, Valparaíso, Chile*

[b] *Physics Division, National Technical University of Athens, 15780 Zografou Campus, Athens, Greece*

*E-mail:* xmeikuang@gmail.com, lpapa@central.ntua.gr

Abstract: We study the holographic dual description of a superconductor in which the gravity sector consists of a Maxwell field and a charged scalar field which except its minimal coupling to gravity it is also coupled kinematically to Einstein tensor. As the strength of the new coupling is increased, the critical temperature below which the scalar field condenses is lowering, the condensation gap decreases faster than the temperature, the width of the condensation gap is not proportional to the size of the condensate and at low temperatures the condensation gap tends to zero for the strong coupling. These effects which are the result of the presence of the coupling of the scalar field to the Einstein tensor in the gravity bulk, provide a dual description of impurities concentration in a superconducting state on the boundary.

Keywords: AdS-CFT Correspondence, Holography and condensed matter physics (AdS/CMT)

ArXiv ePrint: 1607.04928



doi:10.1007/JHEP08(2016)161

JHEP08(2016)161

## Contents



## 1 Introduction

Employing the AdS/CFT correspondence it was shown [1] that a holographic superconductor can be builded on a boundary of a gravity theory consisting of a black hole which acquires scalar hair at temperature below a critical temperature, while above the critical temperature there is no scalar hair. A condensate of the charged scalar field is formed through its coupling to a Maxwell field of the gravity sector. The study was carried out in the probe limit [2], in which in general the product of the charge of the black hole and the charge of the scalar field is held fixed while the latter is taken to infinity and this resulted to neither field to backreact on the metric. Considering fluctuations of the vector potential, the frequency dependent conductivity was calculated, and it was shown that it develops a gap determined by the condensate.

This model was further studied [3] beyond the probe limit. If the scalar charge is large then the backreaction of the scalar field to the spacetime metric has to be considered. It was found that all the basic characteristics of the dual superconductor were persisting even for very small charge. One of the characteristics of these models is the strong pairing mechanism which is in operation. This is due to strong bounding of Cooper pairs and this is manifest to the high values of the gap at low temperature. This strong pairing mechanism resulted to $2\Delta \approx 8.4T_c$, where $\Delta$ is the condensation gap, which has to be compared to the BCS prediction $2\Delta \approx 3.54T_c$, which is much lower in real materials, due to impurities. The above proposals have inspired much effort on further research and on their possible extensions (see [4, 5] and references therein for a review).

The effects of paramagnetic impurities on superconductors were studied in [6]. It was found that the transition temperature decreases sharply with increasing impurity concentration and goes to zero at a critical concentration. Measurements of the energy gap and of the transition temperature $T_c$ as a function of the concentration of paramagnetic impurities



JHEP08(2016)161

show that the gap decreases much more rapidly than does the critical temperature which agrees with the results of [6]. This behaviour was also observed in [7] and [8].

Further calculations on the effects of paramagnetic impurities in superconductors were carried out in [9], taking full advantage of the information contained in the Green's function of the system. The density of states in energy has been computed for different values of the inverse collision time. The excitation energy gap $\Omega_g$ is defined to be the energy at which the density of states vanishes. The temperature-dependent order parameter has been computed and the behaviour of $\Omega_g(T)$ was determined. A comparison with tunneling experiments showed a disagreement of the two parameters. The real part of the conductivity at $T = 0$ is shown to be zero for frequencies less than $2\Omega_g$ and proportional to the square of the density of states for vanishingly small frequencies in the gapless region of impurity concentrations. These detailed calculations showed clearly that in real materials, the essential feature of superconductivity is the correlation of the electrons and the formation of Cooper pairs, rather than the existence of a gap in the excitation energy spectrum. For even in the absence of a gap, so long as correlations persist there is an ordered state below a certain critical temperature which displays the usual properties of a superconductor.

A holographic realization of impurities was discussed in [10]. Using the AdS/CFT correspondence two different types of impurities were calculated and the Nernst response for the impure theory was specified. A model of a gravity dual of a gapless superconductor was proposed in [11]. The gravity sector was consisting of a charged scalar field which provided the scalar hair of an exact black hole solution [12–14] below a critical temperature $T_c$, while an electromagnetic perturbation of the background determined the conductivity giving rise to a gapless superconductor. It was found that the normal component of the DC conductivity had a milder behaviour than the dual superconductor in the case of a black hole of flat horizon [1] in which $n_n$ exhibited a clear gap behaviour. The behaviour it was observed in the boundary conducting theory was attributed to materials with paramagnetic impurities as it was discussed in [9]. Impurities effects were studied in [15], while impurities in the Kondo Model were considered in [16, 17].

In this work we extend the model in [1] by introducing a derivative coupling of the scalar field to Einstein tensor. This term belongs to a general class of scalar-tensor gravity theories resulting from the Horndeski Lagrangian [18]. These theories, which were recently rediscovered [19], give second-order field equations and contain as a subset a theory which preserves classical Galilean symmetry [20–22]. The derivative coupling of the scalar field to Einstein tensor introduces a new scale in the theory which on short distances allows to find black hole solutions [23–27] with scalar hair just outside the black hole horizon, while if one considers the gravitational collapse of a scalar field coupled to the Einstein tensor then the formation of a black hole takes more time to be formed compared to the collapse of a scalar field minimally coupled to gravity [28]. On large distances the presence of the derivative coupling acts as a friction term in the inflationary period of the cosmological evolution [29–31]. Moreover, it was found that at the end of inflation in the preheading period, there is a suppression of heavy particle production as the derivative coupling is increased. This was attributed to the fast decrease of kinetic energy of the scalar field due to its wild oscillations [32].

The above discussion indicates that one of the main effects of the kinematic coupling of a scalar field to Einstein tensor is that gravity influences strongly the propagation of



JHEP08(2016)161

the scalar field compared to a scalar field minimally coupled to gravity. We are going to use this behaviour of the scalar field to holographically simulate the effects of a high concentration of impurities in a material. The presence of impurities in a superconductor is making the pairing mechanism of forming Cooper pairs less effective and this is happening because the quasiparticles are loosing energy because of strong concentration of impurities. This holographic correspondence is supported by our finding. We found that as the value of the derivative coupling is increased the critical temperature is degreasing while the condensation gap $\Delta$ is decreasing faster than the temperature. Also by calculating the perturbation of the scalar potential we found that the condensation gap for large values of the derivative coupling is not proportional to the frequency of the real part of conductivity which is characteristic of a superconducting state with impurities.[1]

The work is organized as follows. In section 2 we review the basic ingredients of the holographic model discussed in [1]. In section 3 we extend the holographic model of section 2 adding a scalar field coupled to Einstein tensor and we give the equations of motion. In section 3.1 we solve numerically the equations of motion and we find the condensation gap and the critical temperature for various values of the derivative coupling. In section 3.2 we study the conductivity while in section 4 are our conclusions.

## 2 Holographic superconductor with a scalar field minimally coupled to gravity

In this section we review in brief the holographic model of [1]. To introduce the minimal holographic superconductor model, we consider a Maxwell field and a charged complex scalar field coupled to gravity with the action

$$S=\int d^4x\sqrt{-g}\left[\frac{R+\Lambda}{16\pi G}-\frac{1}{4}F_{\mu\nu}F^{\mu\nu}-|\nabla\psi-iqA\psi|^2-m^2|\psi|^2\right]. \tag{2.1}$$

If we rescale the fields and the coupling constant as

$$A_\mu=\frac{\tilde{A}_\mu}{q}\,,\quad \psi=\frac{\tilde{\psi}}{q}\,, \tag{2.2}$$

then the matter action in (2.1) has a $1/q^2$ in front, so the backreaction of the matter fields on the metric is suppressed when $q$ is large and the limit $q\to\infty$ defines the probe limit. In this limit the Einstein equations admit as a solution the planar Schwarzschild AdS black hole

$$ds^2=-f(r)dt^2+\frac{dr^2}{f(r)}+r^2(dx^2+dy^2)\,,\qquad f(r)=r^2-\frac{r_h^3}{r}\,. \tag{2.3}$$

Taking the ansatz $\psi=|\psi|$, $A=\phi dt$ where $\psi$, $\phi$ are both functions of $r$ only, we can obtain the equations of motion for $\psi,\phi$

$$\psi''+\left(\frac{f'}{f}+\frac{d-2}{r}\right)\psi'+\left(\frac{\phi^2}{f^2}-\frac{m^2}{f}\right)\psi=0\,, \tag{2.4}$$

[1]We note that in [33] a holographic superconductor was considered containing a derivative coupling for a scalar field in the background of a regular phantom plane symmetric black hole.



JHEP08(2016)161

$$\phi'' + \frac{d-2}{r}\phi' - \frac{2\psi^2}{f}\phi = 0\,. \tag{2.5}$$

It was argued in [2] that there is a critical temperature below which the black hole acquires hair [1, 3].

The equations (2.4) and (2.5) can be solved numerically by doing integration from the horizon out to the infinity taking under consideration the right boundary conditions. The solutions behave like

$$\psi = \frac{\psi_-}{r^{\lambda_-}} + \frac{\psi_+}{r^{\lambda_+}}\,, \qquad \phi = \mu - \frac{\rho}{r}\,, \tag{2.6}$$

with

$$\lambda_\pm = \frac{1}{2}\left[3 \pm \sqrt{(9 + 4m^2L^2)}\,\right], \tag{2.7}$$

where $L$ is the scale of the AdS space and $\mu$ and $\rho$ are interpreted as the chemical potential and charge density in the dual field theory respectively. The coefficients $\psi_-$ and $\psi_+$ according to the AdS/CFT correspondence, correspond to the vacuum expectation values $\psi_- = \langle\mathcal{O}_-\rangle/\sqrt{2}$, $\psi_+ = \langle\mathcal{O}_+\rangle/\sqrt{2}$ of an operator $\mathcal{O}$ dual to the scalar field. We can impose boundary conditions that either $\psi_-$ or $\psi_+$ vanishes.

Fluctuations of the vector potential $A_x$ in the gravity sector gives the conductivity in the dual CFT as a function of frequency. The Maxwell equation for zero spatial momentum and with a time dependence of the form $e^{-i\omega t}$ reads as

$$A_x'' + \frac{f'}{f}A_x' + \left(\frac{\omega^2}{f^2} - \frac{2\psi^2}{f}\right)A_x = 0\,. \tag{2.8}$$

The above equation can be solved by imposing ingoing wave boundary conditions at the horizon $A_x \propto f^{-i\omega/3r_0}$. On the other hand, the asymptotic behaviour of the Maxwell field at boundary is

$$A_x = A_x^{(0)} + \frac{A_x^{(1)}}{r} + \cdots\,. \tag{2.9}$$

Then according to AdS/CFT correspondence dual source and expectation value for the current are given by

$$A_x = A_x^{(0)}\,, \qquad \langle J_x\rangle = A_x^{(1)}\,. \tag{2.10}$$

Finally, Ohm's law gives the conductivity

$$\sigma(\omega) = \frac{\langle J_x\rangle}{E_x} = -\frac{\langle J_x\rangle}{\dot{A}_x} = -\frac{i\langle J_x\rangle}{\omega A_x} = -\frac{iA_x^{(1)}}{\omega A_x^{(0)}}\,. \tag{2.11}$$

## 3 Holographic superconductor with a scalar field kinematically coupled to Einstein tensor

In this section, we will consider a complex scalar field which except its coupling to curvature it is also coupled to Einstein tensor with action

$$I = \int d^4x\sqrt{-g}\left[\frac{R+\Lambda}{16\pi G} - \frac{1}{4}F_{\mu\nu}F^{\mu\nu} - (g^{\mu\nu} + \kappa G^{\mu\nu})D_\mu\psi(D_\nu\psi)^* - m^2|\psi|^2\right], \tag{3.1}$$



JHEP08(2016)161

where

$$D_\mu = \nabla_\mu - ieA_\mu \tag{3.2}$$

and $e$, $m$ are the charge and the mass of the scalar field and $\kappa$ the coupling of the scalar field to Einstein tensor of dimension length squared. For convenience we set

$$\Phi_{\mu\nu} \equiv D_\mu\psi(D_\nu\psi)^* \,, \tag{3.3}$$

$$\Phi \equiv g^{\mu\nu}\Phi_{\mu\nu} \,, \tag{3.4}$$

$$C^{\mu\nu} \equiv g^{\mu\nu} + \kappa G^{\mu\nu} \,. \tag{3.5}$$

The field equations resulting from the action (3.1) are

$$G_{\mu\nu} + \Lambda g_{\mu\nu} = 8\pi T_{\mu\nu} \,, \qquad T_{\mu\nu} = T^{(\psi)}_{\mu\nu} + T^{(EM)}_{\mu\nu} + \kappa\Theta_{\mu\nu} \,, \tag{3.6}$$

where,

$$T^{(\psi)}_{\mu\nu} = \Phi_{\mu\nu} + \Phi_{\nu\mu} - g_{\mu\nu}(g^{ab}\Phi_{ab} + m^2|\psi|^2) \,, \tag{3.7}$$

$$T^{(EM)}_{\mu\nu} = F_\mu{}^\alpha F_{\nu\alpha} - \frac{1}{4}g_{\mu\nu}F_{\alpha\beta}F^{\alpha\beta} \,, \tag{3.8}$$

and

$$\begin{aligned}\Theta_{\mu\nu} = {} & -g_{\mu\nu}R^{ab}\Phi_{ab} + R_\nu{}^a(\Phi_{\mu a} + \Phi_{a\mu}) + R_\mu{}^a(\Phi_{a\nu} + \Phi_{\nu a}) - \frac{1}{2}R(\Phi_{\mu\nu} + \Phi_{\nu\mu}) \\ & -G_{\mu\nu}\Phi - \frac{1}{2}\nabla^a\nabla_\mu(\Phi_{a\nu} + \Phi_{\nu a}) - \frac{1}{2}\nabla^a\nabla_\nu(\Phi_{\mu a} + \Phi_{a\mu}) + \frac{1}{2}\Box(\Phi_{\mu\nu} + \Phi_{\nu\mu}) \\ & +\frac{1}{2}g_{\mu\nu}\nabla_a\nabla_b(\Phi^{ab} + \Phi^{ba}) + \frac{1}{2}(\nabla_\mu\nabla_\nu + \nabla_\nu\nabla_\mu)\Phi - g_{\mu\nu}\Box\Phi \,.\end{aligned} \tag{3.9}$$

The Klein-Gordon equation is

$$(\partial_\mu - ieA_\mu)\left[\sqrt{-g}C^{\mu\nu}(\partial_\nu - ieA_\nu)\psi\right] = \sqrt{-g}m^2\psi \,, \tag{3.10}$$

while the Maxwell equations read

$$\nabla_\nu F^{\mu\nu} + C^{\mu\nu}\left[2e^2A_\nu|\psi|^2 + ie(\psi^*\nabla_\nu\psi - \psi\nabla_\nu\psi^*)\right] = 0 \,. \tag{3.11}$$

### 3.1 Solution of equations of motion and phase transition

As in [1] we also take the ansatz $\psi = |\psi|$, $A = \phi dt$ where $\psi$, $\phi$ are both functions of $r$ only. In the probe limit, under the metric (2.3), the above equations of motion for the matter fields become

$$\begin{aligned}\left[1 + \kappa\left(\frac{f}{r^2} + \frac{f'}{r}\right)\right]\psi'' + \left[\frac{2}{r} + \frac{f'}{f} + \kappa\left(\frac{3f'}{r^2} + \frac{f'^2}{rf} + \frac{f''}{r}\right)\right]\psi' + \\ + \left[\frac{e^2\phi^2}{f^2}\left(1 + \kappa\left(\frac{f}{r^2} + \frac{f'}{r}\right)\right) - \frac{m^2}{f}\right]\psi = 0 \,,\end{aligned} \tag{3.12}$$

$$\phi'' + \frac{2}{r}\phi' - \frac{2e^2\psi^2}{f}\left[1 + \kappa\left(\frac{f}{r^2} + \frac{f'}{r}\right)\right]\phi = 0 \,. \tag{3.13}$$



JHEP08(2016)161

| $\kappa$ | -0.01 | 0 | 0.01 | 0.05 | 0.1 | 0.5 | 1 |
|---|---|---|---|---|---|---|---|
| $\frac{T_c}{\sqrt{\rho}}$ | 0.1218 | 0.1184 | 0.1158 | 0.1091 | 0.1043 | 0.09353 | 0.0906 |
| $C_1$ | 243 | 140 | 73 | 10 | 2 | 0.01 | 0.003 |

**Table 1**. Critical temperature $T_c$ for the phase transition of $\langle O_+ \rangle$ with different $\kappa$.

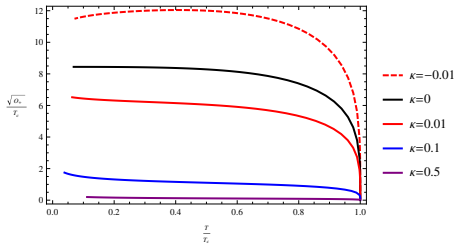


**Figure 1**. The strength of condensation VS the temperature with samples of $\kappa$.

Note that if $\kappa = 0$ then we get the equations (2.4) and (2.5). The new equations depend now on the second derivative of the function $f$ in contrast to the preview case where we had only its first derivative, due to the additional term of $G^{\mu\nu}$ in the action (3.1).

With the same study in the minimal case presented in previous section, we can numerically solve the above equations of motion. We especially study the effect of $\kappa$ on the critical temperature and strength of condensation in the dual superconductor. Without loss of generality, we set $e = 1$ and $m^2 = -2$, so that we have $\lambda_- = 1$ while $\lambda_+ = 2$. We will choose $\psi_-$ as the source which is set to be vanishing, while $\psi_+$ as vacuum expectation values.

The critical temperatures with different $\kappa$ are summarized in table 1. It shows that as the coupling becomes stronger, the critical temperature is lower, meaning that the phase transition is hard to occur as it is expected. This effect of coupling is very different from the influence of higher-derivative coupling between the matters studied in [34, 35]. As the temperature is decreased, the scalar field can have non-zero solution and the strength of condensation becomes higher. We show this phenomena in figure 1. It is obvious that the strength of condensation is suppressed by the derivative coupling. And with enlarging the coupling,[2] the condensation decreases faster than the temperature, so that the condensation gap tends to be zero at low temperatures for the strong coupling. This behaviour from $\kappa$ is coincident with the effect of paramagnetic impurities on superconductors observed in [6–8].

We fit the curve near the critical temperatures. As $T \to T_c$, the condensation is continuous and behaves as

$$\langle \mathcal{O}_+ \rangle \simeq C_1 T_c^2 (1 - T/T_c)^{1/2} \tag{3.14}$$

[2]There is an instability in our numerical solution of the equations of motion for large or small values of the derivative coupling when the temperature is far way from $T_c$. Specially, it is difficult to reach a low temperature $T/T_c \sim 0.1$ when $\kappa > 0.5$. For this reason in figure 1 we restricted the curves to the values of $\kappa$ in the range $-0.01 \leqslant \kappa \leqslant 0.5$. However, when we are near $T_c$ our numerics work better, so we could fit relation (3.14) for larger values of $\kappa$. So in order to study the same shift from the critical temperature in the following study we focus on the range $-0.01 \leqslant \kappa \leqslant 0.5$.



JHEP08(2016)161

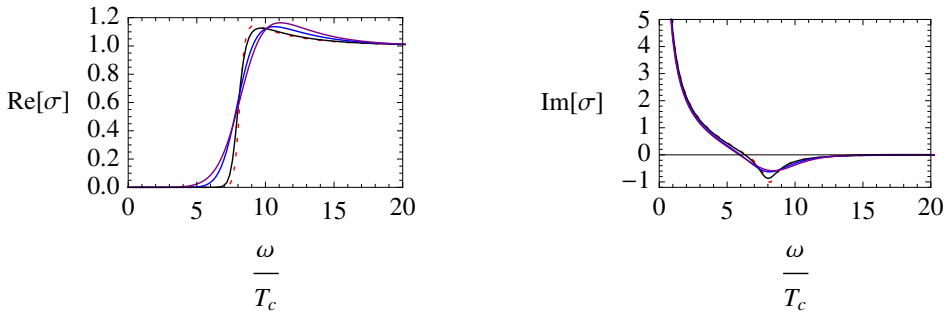


**Figure 2**. Conductivity for samples of $\kappa$ at $T/T_c \simeq 0.1$. The values of $\kappa$ are $\kappa = -0.01$(dotted red),$\kappa = 0$(black),$\kappa = 0.1$(blue) and $\kappa = 0.5$(purple).

where $C_1$ are also listed in table 1. We see that the coefficient $C_1$ decreases drastically to suppress the condensation when the coupling is increased. Observe that the exponent is always 1/2 which implies that $\kappa$ does not modify the order of the phase transition and it is always second order. In the next subsection we will study the conductivity caused by the condensation below the critical temperature.

### 3.2 Conductivity

To compute the conductivity in the dual CFT as a function of frequency we need to solve the Maxwell equation for fluctuations of the vector potential $A_x$. The Maxwell equation at zero spatial momentum and with a time dependence of the form $e^{-i\omega t}$ gives

$$A_x'' + \frac{f'}{f}A_x' + \left[\frac{\omega^2}{f^2} - \frac{2e^2\Psi^2}{f}\left(1 + \kappa\left(\frac{f''}{2} + \frac{f'}{r}\right)\right)\right]A_x = 0\,. \tag{3.15}$$

We will solve the perturbed Maxwell equation with ingoing wave boundary conditions at the horizon, i.e., $A_x \propto f^{-i\omega/3r_0}$. The asymptotic behaviour of the Maxwell field at large radius is $A_x = A_x^{(0)} + \frac{A_x^{(1)}}{r} + \cdots$. Then, according to AdS/CFT dictionary, the dual source and expectation value for the current are given by $A_x = A_x^{(0)}$ and $\langle J_x\rangle = A_x^{(1)}$, respectively. Thus, similar to the equation (2.11), the conductivity is also read as

$$\sigma(\omega) = -\frac{iA_x^{(1)}}{\omega A_x^{(0)}}\,. \tag{3.16}$$

The numerical results of conductivity at low temperature with $\frac{T}{T_c} \simeq 0.1$ are shown in figure 2. Similarly, due to the Kramers-Kronig(KK) relations

$$\mathrm{Im}[\sigma(\omega)] = -\frac{1}{\pi}\mathcal{P}\int_{-\infty}^{\infty}\frac{\mathrm{Re}[\sigma(\omega')]}{\omega' - \omega}d\omega'\,, \tag{3.17}$$

where $\mathcal{P}$ denotes the Cauchy principal value, the divergence of the imaginary part at zero frequency indicates a delta function of real part at $\omega = 0$. At very low temperature, the energy gap in the real part of the conductivity measured by the critical temperature (left



JHEP08(2016)161

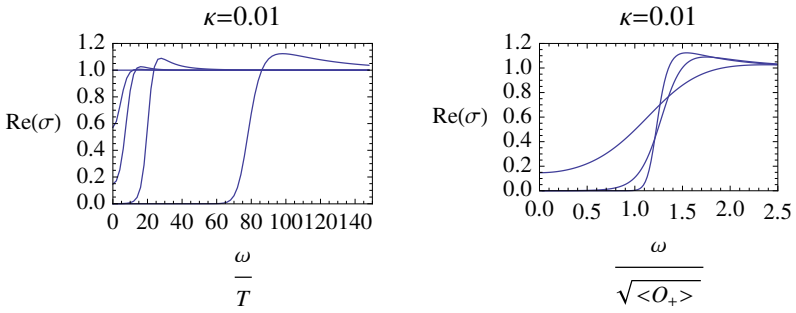


**Figure 3**. Conductivity with $\kappa = 0.01$ as the temperature goes further away from the critical point. In the left plot, from left to right, the temperatures are $T/T_c = 1$, $T/T_c \simeq 0.94$, $T/T_c \simeq 0.80$, $T/T_c \simeq 0.40$, $T/T_c \simeq 0.10$. They are $T/T_c \simeq 0.80$, $T/T_c \simeq 0.40$, $T/T_c \simeq 20$ in the right plot.

| $\kappa$ | -0.01 | 0 | 0.01 | 0.05 | 0.1 | 0.5 |
|---|---|---|---|---|---|---|
| $\frac{\omega_g}{\sqrt{\langle O_+\rangle}}$ | 0.61 | 0.80 | 1 | 1.9 | 2.7 | 20 |

**Table 2**. $\frac{\omega_g}{\sqrt{\langle O_+\rangle}}$ far away from the critical temperature ($T/T_c \simeq 0.10$) with different $\kappa$.

part of figure 2) decreases as the derivative coupling becomes stronger, which agrees well with the behaviour of the condensation as it is depicted in figure 1 in the last subsection.

In order to show how the conductivity opens a gap as the temperature decreases, in figure 3, we show the frequency-dependent conductivity with $\kappa = 0.01$ at different temperatures. In the left plot, the horizontal line, which is frequency independent, corresponds to temperatures at or above the critical value and there is no condensate. As we lower the temperature in the subsequent curves, we see that a gap $\omega_g$ opens in the real part of the conductivity and the gap becomes wider and deeper as the temperature becomes smaller. In the right plot, we plot the conductivity for temperature lower than $T_c$ related the left plot by rescaling the frequency by the condensate. It is obvious that the curves tend to a limit in which the width of the gap is proportional to the size of the condensate. i.e., $\omega_g \simeq \sqrt{\langle O_+\rangle}$. The above features are similar with those in minimal coupling disclosed in [1].

Furthermore, the frequency-dependent conductivity with $\kappa = 0.5$ at different temperatures is presented in figure 4. Similarly to the cases with $\kappa = 0.01$ and minimal coupling, lower temperature gives us wider energy gap. By comparing the left plots of figure 3 and figure 4, we see that at the same scaled temperature $T/T_c$, the gap is narrower for larger coupling, which is consistent with the results shown in figure 1 and figure 2. However, if being scaled by the condensation, see the right plot for $\kappa = 0.5$, the behavior $\omega_g \simeq \sqrt{\langle O_+\rangle}$ at low $T/T_c$ is violated and it is $\omega_g \simeq 20\sqrt{\langle O_+\rangle}$ for $T/T_c \simeq 0.1$. The coefficient 20 is not out of expect. Because if we see carefully the condensation plot figure 1 and figure 2, we will find $\sqrt{\langle O_+\rangle} \simeq 0.2T_c$ and $\omega_g \simeq 4T_c$, so we get the same relation as before $\omega_g \simeq 20\sqrt{\langle O_+\rangle}$.

For the systems far away from the critical temperature ($T/T_c \simeq 0.10$), by careful study, we summarize the values of $\frac{\omega_g}{\sqrt{\langle O_+\rangle}}$ with some $\kappa$ in table 2. It is obvious that as $|\kappa|$ shifts from the minimal coupling, the relation $\omega_g \simeq \sqrt{\langle O_+\rangle}$ is sharply violated, which is one of the



JHEP08(2016)161

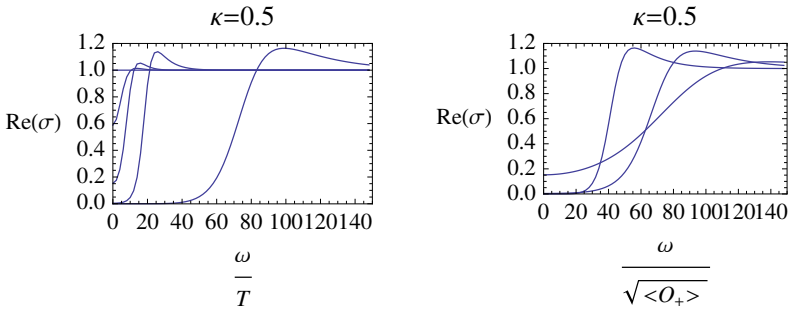


**Figure 4**. Conductivity for $\kappa = 0.5$ with the frequency rescaled by temperature and the condensation. In the left plot, from left to right, the temperatures are $T/T_c = 1$, $T/T_c \simeq 0.94$, $T/T_c \simeq 0.80$, $T/T_c \simeq 0.40$, $T/T_c \simeq 0.10$. They are $T/T_c \simeq 0.80$, $T/T_c \simeq 0.40$, $T/T_c \simeq 0.10$ in the right plot.

main features of a superconducting state with impurities. Note that this effect of possible impurity parameter $\kappa$ is different from that studied in [15] where it can not introduce this kind of violation.

We can now explore the behaviour of conductivity at very low frequency. When $T < T_c$, the real part of the conductivity present a delta function at zero frequency and the imaginary part has a pole, which is attributed to the KK relations (3.17). More specifically, as $\omega \to 0$, the imaginary part behaves as $Im(\sigma) \sim n_s/\omega$, and according to Kramers-Kronig relations, the real part has the form $Re(\sigma) \sim \pi n_s \delta(\omega)$. Here the coefficient $n_s$ of the delta function is defined as the superfluid density. By fitting data near the critical temperature, we find that with various couplings, the superfluid density has the behaviour

$$n_s \simeq C_2 T_c (1 - T/T_c)\,, \tag{3.18}$$

which means that $n_s$ will vanish linearly as $T$ goes to $T_c$. This is consistent with that happens in the minimal coupling. Also we find that the coefficient $C_2$ is not very sensitive to the coupling and the value oscillates around 24 with $\pm 2$ shifting for the samples of $\kappa$. This insensitivity to the changes of the coupling is reasonable because in the region very close to the critical temperature, the system is marginally shifted from the normal state, so that varying $\kappa$ has very small effect on the behaviour of the solutions. Meanwhile, as proposed in [1], the non-superconducting density can be defined as $n_n = \lim_{\omega\to 0} Re(\sigma)$. Far from the critical temperature (with $T/T_c \sim 0.1$), we fit and obtain that $n_n$ decays as

$$n_n \sim \exp\left[-\frac{\Omega_g}{T}\right]\,, \tag{3.19}$$

where $\Omega_g$ can be explained as the energy gap for charged excitation at the corresponding temperature. The values of $\Omega_g$ close to $T/T_c \sim 0.1$ are summarized in table 3. Rough comparison with the numerical energy gap $\omega_g/T_c$ shown in the left plot of figure 2 gives us that $\omega_g \simeq 2\Omega_g$, where the factor 2 suggests that the gaped charged quasiparticles are formed in pairs as addressed in [1]. Analyzing the data in the table, we see that $\kappa = 0.5$ corresponds to $\omega_g \simeq 2\Omega_g \simeq 4T_c$ which is very near the prediction $\omega_g \simeq 3.54T_c$ in BCS theory.



JHEP08(2016)161

| $\kappa$ | -0.01 | 0 | 0.01 | 0.05 | 0.1 | 0.5 |
|---|---|---|---|---|---|---|
| $\frac{\Omega_g}{T_c}$ | 4.0 | 3.8 | 3.5 | 3.0 | 2.8 | 2.0 |

**Table 3**. The energy gap for charged excitation $\frac{\Omega_g}{T_c}$ with different $\kappa$.

In this tendency, we believe that BCS prediction may be fulfilled by larger coupling once the numerics are controlable. Thus, in this sense, the derivative coupling somehow mimic the effect of the impurities in a real material.

## 4 Conclusions

We studied a holographic description of a superconductor in which the gravity sector consists of a Maxwell field and a charged scalar field which except its usual minimal coupling to gravity it is also coupled to Einstein tensor. Solving the equations of motion numerically in the probe limit, we found that as the strength of the new coupling is increased, the critical temperature below which the scalar field condenses is lowering, the condensation gap decreases faster than the temperature, the width of the condensation gap is not proportional to the size of the condensate and at low temperatures the condensation gap tends to zero for the strong coupling. Analysing the frequency dependence of conductivity we found that at strong coupling the relation $\omega_g \simeq 2\Omega_g \simeq 4T_c$ holds, where $\Omega_g$ is the energy gap for charged excitation, which is very near the prediction $\omega_g \simeq 3.54T_c$ in BCS theory.

We argued that these results suggest that the derivative coupling in the gravity bulk can have a dual interpretation on the boundary corresponding to impurities concentrations in a real material. This correspondence can be understood from the fact that the coupling of a scalar field to Einstein tensor alters the kinematical state of the scalar field a behaviour which it is also exhibited by the quasiparticles moving in a material with impurities.

We believe that the probe limit captures all the essential features of the problem under study. Nevertheless, it would be interesting to extend this study beyond the probe limit. Assuming a spherically symmetric ansatz for the metric the field equations (3.6), (3.10) and (3.11) have to be solved. However, even their numerical solution is a formidable task mainly because of the presence of the energy-momentum tensor (3.9) resulting from the coupling of the scalar field to Einstein tensor. A more realistic approach would be to follow the perturbative methods employed in [23, 25].

## Acknowledgments

We thank Olivera Miskovic and George Filios for their contribution at the early stage of this work. X-M.K is partly supported by FONDECYT Grant No.3150006.





JHEP08(2016)161

## References


[1] S.A. Hartnoll, C.P. Herzog and G.T. Horowitz, *Building a holographic superconductor*, *Phys. Rev. Lett.* **101** (2008) 031601 [arXiv:0803.3295] [INSPIRE].

[2] S.S. Gubser, *Breaking an Abelian gauge symmetry near a black hole horizon*, *Phys. Rev.* **D 78** (2008) 065034 [arXiv:0801.2977] [INSPIRE].

[3] S.A. Hartnoll, C.P. Herzog and G.T. Horowitz, *Holographic superconductors*, *JHEP* **12** (2008) 015 [arXiv:0810.1563] [INSPIRE].

[4] G.T. Horowitz, *Introduction to holographic superconductors*, *Lect. Notes Phys.* **828** (2011) 313 [arXiv:1002.1722] [INSPIRE].

[5] R.-G. Cai, L. Li, L.-F. Li and R.-Q. Yang, *Introduction to holographic superconductor models*, *Sci. China Phys. Mech. Astron.* **58** (2015) 060401 [arXiv:1502.00437] [INSPIRE].

[6] A.A. Abrikosov and L.P. Gor'kov, *Contribution to the theory of superconducting alloys with paramagnetic impurities*, *Sov. Phys. JETP* **12** (1961) 1243 [*Zh. Eksp. Teor. Fiz.* **39** (1961) 1781].

[7] G. de Gennes and G. Sarma, *Some relations between superconducting and magnetic properties*, *J. Appl. Phys.* **34** (1963) 1380.

[8] J.C. Phillips, *Gapless superconductivity*, *Phys. Rev. Lett.* **10** (1963) 96.

[9] S. Skalski, O. Betbeder-Matibet and P.R. Weiss, *Properties of superconducting alloys containing paramagnetic impurities*, *Phys. Rev.* **136** (1964) A1500.

[10] S.A. Hartnoll and C.P. Herzog, *Impure AdS/CFT correspondence*, *Phys. Rev.* **D 77** (2008) 106009 [arXiv:0801.1693] [INSPIRE].

[11] G. Koutsoumbas, E. Papantonopoulos and G. Siopsis, *Exact gravity dual of a gapless superconductor*, *JHEP* **07** (2009) 026 [arXiv:0902.0733] [INSPIRE].

[12] C. Martinez, R. Troncoso and J. Zanelli, *Exact black hole solution with a minimally coupled scalar field*, *Phys. Rev.* **D 70** (2004) 084035 [hep-th/0406111] [INSPIRE].

[13] C. Martinez, J.P. Staforelli and R. Troncoso, *Topological black holes dressed with a conformally coupled scalar field and electric charge*, *Phys. Rev.* **D 74** (2006) 044028 [hep-th/0512022] [INSPIRE].

[14] C. Martinez and R. Troncoso, *Electrically charged black hole with scalar hair*, *Phys. Rev.* **D 74** (2006) 064007 [hep-th/0606130] [INSPIRE].

[15] T. Ishii and S.-J. Sin, *Impurity effect in a holographic superconductor*, *JHEP* **04** (2013) 128 [arXiv:1211.1798] [INSPIRE].

[16] A. O'Bannon, I. Papadimitriou and J. Probst, *A holographic two-impurity Kondo model*, *JHEP* **01** (2016) 103 [arXiv:1510.08123] [INSPIRE].

[17] J. Erdmenger, M. Flory, C. Hoyos, M.-N. Newrzella, A. O'Bannon and J. Wu, *Holographic impurities and Kondo effect*, *Fortsch. Phys.* **64** (2016) 322 [arXiv:1511.09362] [INSPIRE].

[18] G.W. Horndeski, *Second-order scalar-tensor field equations in a four-dimensional space*, *Int. J. Theor. Phys.* **10** (1974) 363 [INSPIRE].

[19] C. Deffayet, X. Gao, D.A. Steer and G. Zahariade, *From k-essence to generalised Galileons*, *Phys. Rev.* **D 84** (2011) 064039 [arXiv:1103.3260] [INSPIRE].


JHEP08(2016)161

[20] A. Nicolis, R. Rattazzi and E. Trincherini, *The Galileon as a local modification of gravity*, *Phys. Rev.* **D 79** (2009) 064036 [arXiv:0811.2197] [INSPIRE].

[21] C. Deffayet, G. Esposito-Farese and A. Vikman, *Covariant Galileon*, *Phys. Rev.* **D 79** (2009) 084003 [arXiv:0901.1314] [INSPIRE].

[22] C. Deffayet, S. Deser and G. Esposito-Farese, *Generalized Galileons: all scalar models whose curved background extensions maintain second-order field equations and stress-tensors*, *Phys. Rev.* **D 80** (2009) 064015 [arXiv:0906.1967] [INSPIRE].

[23] T. Kolyvaris, G. Koutsoumbas, E. Papantonopoulos and G. Siopsis, *Scalar hair from a derivative coupling of a scalar field to the Einstein tensor*, *Class. Quant. Grav.* **29** (2012) 205011 [arXiv:1111.0263] [INSPIRE].

[24] M. Rinaldi, *Black holes with non-minimal derivative coupling*, *Phys. Rev.* **D 86** (2012) 084048 [arXiv:1208.0103] [INSPIRE].

[25] T. Kolyvaris, G. Koutsoumbas, E. Papantonopoulos and G. Siopsis, *Phase transition to a hairy black hole in asymptotically flat spacetime*, *JHEP* **11** (2013) 133 [arXiv:1308.5280] [INSPIRE].

[26] A. Cisterna and C. Erices, *Asymptotically locally AdS and flat black holes in the presence of an electric field in the Horndeski scenario*, *Phys. Rev.* **D 89** (2014) 084038 [arXiv:1401.4479] [INSPIRE].

[27] Y. Brihaye, A. Cisterna and C. Erices, *Boson stars in biscalar extensions of Horndeski gravity*, *Phys. Rev.* **D 93** (2016) 124057 [arXiv:1604.02121] [INSPIRE].

[28] G. Koutsoumbas, K. Ntrekis, E. Papantonopoulos and M. Tsoukalas, *Gravitational collapse in Horndeski theory*, arXiv:1512.05934 [INSPIRE].

[29] L. Amendola, *Cosmology with nonminimal derivative couplings*, *Phys. Lett.* **B 301** (1993) 175 [gr-qc/9302010] [INSPIRE].

[30] S.V. Sushkov, *Exact cosmological solutions with nonminimal derivative coupling*, *Phys. Rev.* **D 80** (2009) 103505 [arXiv:0910.0980] [INSPIRE].

[31] C. Germani and A. Kehagias, *UV-protected inflation*, *Phys. Rev. Lett.* **106** (2011) 161302 [arXiv:1012.0853] [INSPIRE].

[32] G. Koutsoumbas, K. Ntrekis and E. Papantonopoulos, *Gravitational particle production in gravity theories with non-minimal derivative couplings*, *JCAP* **08** (2013) 027 [arXiv:1305.5741] [INSPIRE].

[33] K. Lin, A.B. Pavan, Q. Pan and E. Abdalla, *Regular phantom black hole and holography: very high temperature superconductors*, arXiv:1512.02718 [INSPIRE].

[34] X.-M. Kuang, E. Papantonopoulos, G. Siopsis and B. Wang, *Building a holographic superconductor with higher-derivative couplings*, *Phys. Rev.* **D 88** (2013) 086008 [arXiv:1303.2575] [INSPIRE].

[35] X.-M. Kuang, E. Papantonopoulos and B. Wang, *Entanglement entropy as a probe of the proximity effect in holographic superconductors*, *JHEP* **05** (2014) 130 [arXiv:1401.5720] [INSPIRE].

JHEP08(2016)161